KTH Land and Water
Resources Engineering

Hydrological Transport in Shallow Catchments:
tracer discharge, travel time and water age

Sofie S. Soltani

October 2017

TRITA-LWR PhD-2017:10
ISBN 978-91-7729-539-6
ISSN 1650-8602
ISRN KTH/LWR/PHD

PhD thesis
Division of Land and Water Resources Engineering
Department of Sustainable Development, Environmental Science and Engineering
School of Architecture and the Built Environment
Royal Institute of Technology (KTH)
SE-100 44 STOCKHOLM, Sweden
Reference should be written as: Soltani S.S. (2017) "Hydrological Transport in Shallow Catchments: tracer discharge, travel time and water age" TRITA-LWR PhD-2017:10

It was the best of times,
It was the worst of times,
It was the age of wisdom,
It was the age of foolishness,...

Charles Dickens

PREFACE

This doctoral thesis consists of a summarizing text and the four papers listed below.

Paper I **Soltani, S. S.**, and V. Cvetkovic (2013), On the distribution of water age along hydrological pathways with transient flow, *Water Resources Research*, Volume 49, Pages 5238-5245.
SS contributed to the conceptualization, carried out the simulations and writing

Paper II **Soltani, S. S.** and V. Cvetkovic (2017), Quantifying the distribution of tracer discharge from boreal catchments under transient flow using the kinematic pathway approach, *Water Resources Research*, Volume 53, Pages 5659-567.
SS contributed to the conceptualization, carried out the simulations and writing

Paper III Cvetkovic, V., **S. S. Soltani**, and G. Vigouroux (2015), Global sensitivity analysis of groundwater transport, *Journal of Hydrology*, Volume 531, Pages 142-148.
SS contributed to conceptualizations and reviewing the manuscript

Paper IV **S.S. Soltani**, V. Cvetkovic (2017), Contaminant attenuation by shallow aquifer systems under steady flow, *Advances in Water Resources*, Volume 108, Pages 157-169.
SS contributed to the conceptualization, carried out the simulations and writing

SWEDISH SUMMARY

Detta arbete fokuserar på hydrologisk transport i grunda avrinningsområden med topografistyrda flödesvägar . Avhandlingen ger ny insikt i kinematiska flödesmodeller för uppskattning av spårämnesutsläpp vid avrinningsområdesutloppet. En semi-analytisk metod presenteras för transient restid och åldersfördelning kallad ”kinematic pathway approach” (KPA) vilken står för dispersion på två nivåer av morfologisk och makro-dispersion. Macro-dispersion och morfologisk dispersion komponenter reflekteras i KPA genom respektive antagande av ett effektivt Peclet nummer och topografidriven flödesvägslängdsfördelning. Det kinematiska måttet på transporten definierat som en karaktäristisk hastighet av vattenflödet genom avrinningsområdet erhålls från den totala vattenbalansen i avrinningsområdet. För att inkludera transformationsprocess i dess enklaste form av linjärt sönderfall/nedbrytning presenteras ett ramverk som löser endimensionell reaktiv transport med numeriskt simulerade restider som den oberoende variabeln. Den föreslagna KPA samt kopplat transport ramverk för kvantifiering av spårämnesutsläpp vid grunda avrinningsområdesutlopp tillämpas på två valda avrinningsområden i Sverige. KPA tillämpas på modellering av en 23 år lång dataserie för klorid gällande Kringlans avrinningsområde medan tillämpning av ramverket för kvantifiering av naturlig förstärkning är illustrerad för Forsmarks avrinningsområde. Numeriska simuleringar av Forsmarks avrinningsområdes advektiv trasnporttid fås genom partikelspårning i den fullt integrerade flödesmodellen MIKE SHE under stabila flödesförhållanden. KPA bedöms ge rimliga uppskattningar av spridningsfördelningen av spårämnen vid övervägning av transporten som övervägande kontrollerad av hillslope-processer associerade med relativt korta topografiskt drivna flödesvägar till intilliggande utsläppszoner, t.ex. vattendrag och sjöar. Även simulerad naturlig förstärkning i Forsmark är rimligen väl uppskattad förutsatt at resvägslängdsfördelning är tillräckligt snedställd gentemot korta resvägslängder. Detta faktum är en indikation på den kontrollerande inverkan av topografi på flödesvägslängd samt restidsfördelning i grunda avrinningsområden, vilka ligger till grund för det föreslagna kinematiska tillvägagångssättet. Vårt arbete har visat att resvägsmetoderna (Lagrangian) är lovande som prediktiva verktyg för hydrologisk transport. Ytterligare jämförelse mellan kinematiska och dynamiska modeller krävs dock för att mer exakt fånga betydelsen av underjordiska hydrogeologiska strukturer vilka tillsammans med topografin kontrollerar transport.

ACKNOWLEDGMENTS

I gratefully acknowledge the financial support of the Swedish Nuclear Fuel and Waste Management Co. (SKB). I would like to acknowledge my main supervisor, Vladimir Cvetkovic, and co-supervisors Bijan Dargahi and Jan-Olof Selroos. Vladimir, thank you for the life changing opportunity, thank you for our inspirational dialogues, thank you for your trust and for your integrity. I am grateful to Jan-Olof for our many useful discussions: it was my pleasure to complete my studies under your guidance. I am also in great dept to Tim Ginn (Washington State University), my mentor and role model in teaching who always kept an eye on my achievements since our paths crossed. Thank you Tim! I also would like to thank Gia Destouni for our discussions and broadening my horizons in the world of scientific research. And my special thanks to Luigia Brandimarte for the suggestions to the Kappa.

I would like to thank my colleagues and former colleagues at the LWR department at KTH, UC Davis and SU. Thank you for shared academic adventures, laughs and support.

My personal acknowledgments go to Shahla Dargahi, Deena Stanley, Hariss's family who made my stay in Davis unforgettable.

I have had the fortune to come across some very good people over the years of my stay in Stockholm. Pooyeh, Sahand, Farzad and Mj thank you for our moments.

Bijan and Shahrzad, you nourished my life with your morals, compassion and humanity. I am eternally grateful for everything you've taught me.

And finally, I would like to thank my beloved family. Mother, you are my strength. You are my confidence. You are me and I am you. Father, This thesis is a testament to your endless passion for learning. You taught me there is no end to education. Forever in debt! Kamran, Fereshteh and Maryam without you this was not possible. This humble effort is dedicated to you!

Sofie Safeyeh Soltani
Stockholm, October 2017

Contents

List of Figures

List of Tables

ABBREVIATIONS

TTD	Travel Time Distribution
TOSS	Tempered One-Sided Stable
AD	Age Distribution
NAP	Natural Attenuation Potential
KPA	Kinematic Pathway Approach
t	Time [T]
A	Recharge/injection area [L^2]
B	Discharge area [L^2]
$\mathbf{a}$	Recharge/injection location vector [L]
$\mathbf{b}$	Discharge location vector [L]
AB	Pathway between A and B
$\tau(\mathbf{a}, \mathbf{b})$	Travel time between between A and B
$T(A, B)$	Average water travel time of an ensemble of tracer particles injected over A from A to B
$J(t, \tau)$	The tracer mass flux or discharge [M/T/L^2]
$m(t; \mathrm{A}, \mathrm{B})$	Total mass discharged between A and B [M]
PDF	Probability Density Function
CDF	Cumulative Distribution Function
CCDF	Complementary Cumulative Distribution Function
$\phi(t)$	Temporal function [ ]
$U(t)$	Transient mean velocity of [L/T]
$F_{AB}(t; x)$	Travel time CDF for a single pathway AB [ ]
$F_{BA}(t; x, \theta)$	Water age CDF for a single pathway BA [ ]
λ_L	Axial macro-dispersivity [L]
ϕ_b	Inverted temporal variability function
L	Catchment length scale [L]
$P_n(t)$	Net precipitation (precipitation minus evapotranspiration) [L^3/T]
$Q(t)$	Flow discharge from the catchment [L^3/T]
r	Transport pathway length [L]
$F_f(t; L)$	Catchment water travel time CDF [ ]
$p(r)$	Pathway length PDF [1/L]

c_{drain}	Drainage capacity [L^2]
$F_b(t; L, \theta)$	Catchment water age CDF [ ]
U_0	Catchment characteristic velocity [L/T]
$\bar{h}$	Average (or effective) aquifer thickness [L]
$\bar{P}$	Long-term average precipitation [L/T]
$\overline{ET}$	Long-term average actual evapotranspiratio [L/T]
$\overline{PET}$	Long-term average potential evapotranspiratio [L/T]
ζ	Coefficient of variation for τ [ ]
J_0	Continuous tracer input per unit catchment area [M/T/L^2]
$C_0(t)$	Input tracer concentration [M/L^3]
η	Attenuation index [ ]
Pe	Péclet number [ ]
λ	Mass decay rate [1/T]
LT	Laplace Transform
CV	Coefficient of variation

ABSTRACT

This focuses on hydrological transport in shallow catchments with topography-driven flow paths. The thesis gives new insight to kinematic pathway models for estimation of tracer discharge at the catchment outlet. A semi-analytical methodology is presented for transient travel time and age distributions referred to as "kinematic pathway approach“ (KPA) that accounts for dispersion at two levels of morphological and macro-dispersion. Macro-dispersion and morphological dispersion components are reflected in KPA by assuming an effective Péclet number and topographically driven pathway length distributions, respectively. The kinematic measure of the transport, defined as a characteristic velocity of water flow through the catchment is obtained from the overall water balance in the catchment. To include transformation process in its simplest form of linear decay/degradation a framework is presented that solves one-dimensional reactive transport with numerically simulated travel times as the independent variable. The proposed KPA and coupled transport framework for quantifying tracer discharge at the shallow catchment outlet are applied to two selected catchments in Sweden. KPA is applied to modeling of a 23-year long chloride data series for the Kringlan catchment whereas the implantation of the framework for quantifying natural attenuation is illustrated for the Forsmark catchment. Numerical simulations of Forsmark catchment advective travel times are obtained by means of particle tracking using the fully-integrated flow model MIKE SHE under steady-state flow conditions. The KPA is found to provide reasonable estimates of tracer discharge distribution when considering the transport as predominantly controlled by hillslope processes associated with relatively short topographically driven flow paths to adjacent discharge zones, e.g. rivers and lakes. Simulated natural attenuation for Forsmark is also estimated reasonably well provided that the pathway length distribution is sufficiently skewed toward short pathway lengths. This fact is indicative of the controlling impact of topography on flow path length and travel time distributions in shallow catchments, which is the basis of the proposed kinematic pathway approach. Our work has shown that the pathway (Lagrangian) methodologies are promising as predictive tools for hydrological transport. Further comparison between kinematic and dynamic models is needed however to more accurately capture the role of subsurface hydrogeological structures which jointly with topography control transport.

Keywords: Hydrological transport, travel time, water age, tracer discharge, Lagrangian/pathway approach, pathway lengths, numerical modeling

Motion of particle mass within a hydrological system (e.g. catchment) is referred to as hydrological transport and characterized by physical, chemical and biological mechanisms. Tracer discharge, water travel time and age are basic measures of hydrological transport in catchments relevant for diverse applications (Maloszewski & Zuber, 1996; Kirchner *et al.*, 2001; Weissmann *et al.*, 2002; Lindgren *et al.*, 2004; McGuire & McDonnell, 2006; Cardenas, 2007; Troldborg *et al.*, 2008; Bosson *et al.*, 2010; Darracq *et al.*, 2010; Botter *et al.*, 2011; Destouni *et al.*, 2010; McDonnell *et al.*, 2010; Rinaldo *et al.*, 2011; Benettin *et al.*, 2015). The discharge of a dissolved substance (a passive solute, or tracer) at a catchment outlet, defined as mass per unit time, can be characterized by a statistical distribution. The statistical distribution of the tracer discharge, with emphasis on the high value range is important from water quality perspective, for the potential impact of contaminants on aquatic systems, be it fresh or coastal waters (Destouni *et al.*, 2010). Travel time is also an essential measure of transport from a more basic perspective for understanding the interacting catchment structures. Travel time and age are of relevance for a variety of water quality matters such as first arrivals, residence times and potential source-locations of contaminants.

1 Hydrological transport

Hydrological transport is governed by three mechanisms: (i) variable water flow that results in advection and dispersion (referred to as hydrodynamic components), (ii) mass transfer (i.e., exchange with the immobile zones/phase), (iii) mass transformation (e.g. decay/degradation). These three components occur simultaneously, and for a linear system are hierarchical: the hydrodynamic components directly influence mass transfer. Advection-dispersion and mass transfer strongly influence degradation, whereas degradation of a contaminant has no impact on the hydrodynamics or mass transfer; likewise, mass transfer does not influence the hydrodynamics (Cvetkovic *et al.*, 2015).

1.1 Hydrodynamic transport

To understand hydrological transport,a combination of methods should be used starting from observations, characterization methods for acquiring basic data, analytical and conceptual (lumped) models for simpler assessment and interpretation, to numerical physically based models for more detailed evaluation and analysis. Water transport is controlled by the hydrodynamics which in turn is controlled by the catchment structure on the one hand, and boundary conditions on the other. Characterization of the structure, hydraulic properties and boundary conditions is therefore an important step in quantifying water transport, yet it is costly and therefore at best builds on sparse (insufficient) information. Even if a catchment is fully characterized, relating these properties to water transport still requires some type of tracer test (experiment) where both input and output are sufficiently well defined. Ideally, one would like to trace every water molecule that enters a given catchment until its exit but clearly such an experiment is not possible (McDonnell *et al.*, 2010); in reality, there are relatively few cases of tracer data on catchment scales for which input and output are sufficiently well known. Significant observation/experimental gaps therefore need to be closed between detailed characterization of catchment structural and flow properties, to tracer tests that can be used for verifying hypotheses on transport; such gaps are typically closed by some type of modeling.

Models for hydrological transport through catchments can be roughly divided into two categories: *kinematic* and *dynamic* models. The *kinematic models* build on theoretical approaches that ultimately rest on the tracer mass balance assuming the existence of the underlying flow field. Such models may be lumped (or conceptual) and consider a catchment as a systems of interconnected hydrological units, or they may be based on a pathway approach where a statistical distribution is ultimately used (assumed or inferred) to quantify transport. The dynamic models build on numerically resolving the hydrodynamics in a given catchment structure, combining water mass balance and momentum (flow) equations. In this context, numerical simulations are becoming

increasingly important for understanding catchment scale flow and material transport (e.g., Loague & VanderKwaak, 2004). Whereas the kinematic models are relatively simple for implementation and can be easily adjusted to any amount of data, they are difficult to test, both due to lack of tracer data as well as a sufficient link to the structure and boundary conditions. The dynamic models on the other hand always require more information than is available, suffering from problems of scale, sub-grid representation techniques, equifinality and model structural errors (e.g., Beven, 1989, 2001, 2009; Butts *et al.*, 2004; Lindgren & Destouni, 2004; Refsgaard *et al.*, 2006; Darracq & Destouni, 2007). It is clear that further advancement in the quantification of hydrological transport should in some way combine different modeling tools with data in order to bridge the still large gaps between the kinematic and dynamic modeling approaches.

1.1.1 Travel time distribution

To quantify hydrological transport using either kinematic or dynamic models, water (or solute) travel time is the key quantity. Travel time is the transit time from recharge point/area to discharge point/area along the connecting hydrological pathway.

The most general analytical form of travel time distribution (TTD) of kinematic models is the tempered one-sided stable (TOSS) density (Cvetkovic, 2011a) which can be reduced to most of the distributions used for hydrological transport in the literature. Commonly used distributions, such as the "Delta function (Plug flow)", "Gamma," "Exponential (Flow reactor)" and "Inverse-Gaussian", are well discussed in (Małoszewski & Zuber, 1982; Haitjema, 1995; Maloszewski & Zuber, 1996; Rodhe *et al.*, 1996; Kirchner *et al.*, 2000; McGuire & McDonnell, 2006; Kirchner *et al.*, 2001) and applied to specific catchments, using tracer data.

Kinematic pathway models are based on a defined hydrological pathway concept (e.g., Cvetkovic *et al.*, 2012). Hydrodynamic transport is then quantified by aggregation of the transport through pathways of diverse lengths that may cross different hydrological units e.g., aquifers, streams, lakes (Paper II) using a (assumed or inferred) statistical distribution for travel time (Lindgren *et al.*, 2004; Wörman *et al.*, 2006; Cardenas, 2007; Tetzlaff *et al.*, 2009). Commonly, the mean movement of water (or solute) is considered to follow local topographical gradient to a discharge point/area (Toth, 1963; McGuire *et al.*, 2005; Wörman *et al.*, 2006; Cardenas, 2007; Tetzlaff *et al.*, 2009) through topographically-driven pathways.

In dynamic models of hydrological systems, the particle travel times between source point/area to output point/area is typically numerically quantified using the particle tracking modules available in ready-to-use flow and transport simulation tools, e.g., MIKE SHE (Troldborg *et al.*, 2008; Bosson *et al.*, 2010) and MODFLOW (Weissmann *et al.*, 2002; Woolfenden & Ginn, 2009; Goderniaux *et al.*, 2013). One should note that calculated flow velocity field based on hydrological and hydraulic data is a prerequisite for running any particle tracking tools. Alternatively, TTDs are numerically calculated using fully spatially distributed physical models for hydrological transport (Fiori & Russo, 2008; Fiori *et al.*, 2009; Engdahl & Maxwell, 2015).

1.1.2 Water age distribution

The time water particles spent in a hydrological system from a recharge point to an arbitrary location is the water age (Małoszewski & Zuber, 1982; Goode, 1996; Varni & Carrera, 1998; Ginn, 1999; Weissmann *et al.*, 2002). Water age is a transient, spatially distributed physical measure for hydrodynamic transport of relevance for water resources management from both water quantity and quality perspectives. Lumped-parameter models have been in widespread use to evaluate age distribution (AD) or backward TTD from environmental tracers (Małoszewski & Zuber, 1982; Małoszewski *et al.*, 1983; Maloszewski & Zuber, 1996). Kinematic pathway models, on the other hand, are recently introduced by Paper II using a proposed AD by Paper I.

Among particle tracking tools available, only few (e.g., MODFLOW) are capable of applying a backward-time particle tracking approach to simulate AD (Weissmann *et al.*, 2002). The first dynamic models for mean AD in groundwater was proposed by Goode (1996) and further developed by Varni & Carrera (1998). The most general AD model (Ginn, 1999) was numerically implemented for aquifers under steady-state flow (Woolfenden & Ginn, 2009). Later,

Cornaton (2012) developed a novel numerical method for water AD under transient flow condition based on Ginn (1999) theory. Recently, the method was incorporated as age module in FEFLOW, for simulating flow and transport in porous media (*DHI-WASY GmbH*, 2012). However, computation of the solution to the five dimensional (5D) governing equation for AD by Ginn (1999) requires extensive numerical calculations.

1.2 Mass transfer

Mass transfer is a solute transport mechanism between mobile and immobile zones with multiple and simultaneous rates. Originally, multi-rate mass transfer models were introduced for describing the trapping process in different physical systems (e.g., Noolandi, 1977) and later for hydrological transport (Haggerty & Gorelick, 1995; Carrera *et al.*, 1998). Several distributed multi-rate mass transfer models are investigated and summarized by Haggerty *et al.* (2000).

1.3 Mass transformation

Mass transformation in its simplest possible form is linear decay/degradation. Contaminant mass loss over time is decay; whereas, degradation is a biogeochemical process of organic contaminant mass loss over time. The latter is dominated by type of the organic matter, aerobic/anaerobic condition, the presence of other organic and inorganic substances, microbial activities and most importantly hydrodynamic transport. Given the complexity of the bio-chemical details, the degradation process is often simplified as linear decay with fitted (or assumed) decay rate coefficient (e.g., Nielsen *et al.*, 1995; Darracq *et al.*, 2008; Alvarez & Illman, 2005; Destouni *et al.*, 2010).

1.3.1 Attenuation index

The self-purifying capacity of groundwater, i.e. irreversible loss of contaminant mass as a result of coupled transport and transformation processes (here expressed as a first-order loss) is measured by an attenuation index (Cvetkovic, 2011b; Cvetkovic *et al.*, 2015). To summarize, attenuation (mass loss), of real or potential contaminants is a result of all three hydrological transport coupled mechanisms: (i) hydrodynamic drivers, which move and spread a tracer by water flow, (ii) mass transfer, which slows down tracer movement relative to water flow because of an exchange between the mobile and immobile fluid or solid, and (iii) transformation (decay or degradation), which permanently removes a tracer from the system (Paper III).

The quantitative evaluation of "natural attenuation potential" (NAP) of groundwater systems for self-purification (Paper IV) can be of relevance to the ongoing research on the development of groundwater quality in-situ remediation techniques and technological interventions. In the present thesis, a simple framework is proposed for the assessment of NAP of groundwater systems in catchment scale.

2 Aims and objectives

The main research question in this thesis is *When are simple kinematic models applicable for the tracer discharge, travel time and water age distributions in hydrological transport?*

Traditionally, the overwhelming complexity of hydrological transport has led either to relatively simple kinematic models like mixed reactors, or to an attempt to capture complexity explicitly, as dynamic models. The classical kinematic models (Małoszewski & Zuber, 1982; Haitjema, 1995; Maloszewski & Zuber, 1996; Rodhe *et al.*, 1996; Kirchner *et al.*, 2000, 2001; McGuire & McDonnell, 2006) cannot fully differentiate spatially-dependent hydrological transport processes (including flow structure) or reservoirs (e.g. shallow and deep aquifer systems), whereas the dynamic models demand for high-level numerical efforts (Bosson *et al.*, 2010; Weissmann *et al.*, 2002; Troldborg *et al.*, 2008; Fiori & Russo, 2008; Woolfenden & Ginn, 2009; Fiori *et al.*, 2009; Engdahl & Maxwell, 2015). In addition, lack of tracer data (to assume or infer TTD) for kinematic models on one hand and field data for dynamic models on the other hand are limiting factors for large scale applications.

This thesis attempts to bridge the gap between kinematic and dynamic models with the following specific objectives:

1. To propose a simple TTD and AD along 1D hydrological pathways under transient flow, applicable in kinematic models;
2. to develop a kinematic pathway approach

(KPA) based on the proposed simple TTD and link it to the structure and boundary condition for quantifying catchment-scale hydrological transport;

3. to evaluate the KPA by applying it to a real catchment case study with tracer data time-series;

4. to investigate the kinematic models in form of the most general analytical model, TOSS, using the attenuation index as a relevant measure of coupled transport mechanisms;

5. to study the impact of water travel time variability on hydrological transport at two levels: (i) catchment scale and (ii) single pathway (between recharge and discharge zones) scale; and

6. to combine kinematic and dynamic models to address integrated hydrological transport.

The objectives of this thesis are addressed by the appended articles. Paper I presents the development of the simple TTD and AD along 1D hydrological pathways under transient flow in a generic context. Paper II introduces the developed KPA with application to the real catchment case study to quantify catchment-scale temporal statistics of trace discharge in comparison to chloride tracer data. Paper III explores the parametric kinematic models in a general form with attenuation index as the measure. Paper IV discusses the impact of water travel time variations on hydrological transport at different levels of single pathway and entire catchment. It also presents a framework for analyzing coupled hydrological transport (i.e. hydrodynamic transport and transformation) using combined dynamic and kinematic modeling approach. Moreover, it explores if the self-purification potential of a catchment can be simply estimated from basic hydrological data and morphological pathway analysis.

METHODS

This section first describes the theoretical basis of the thesis and summarizes the methods developed to quantify hydrological transport at the catchment scale.

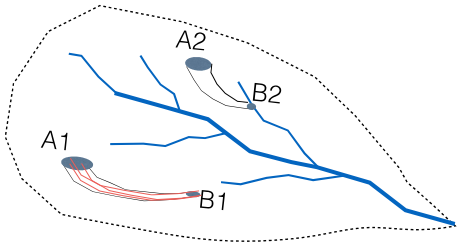

Figure 1: Configuration sketch of pathways A_1B_1 and A_2B_2 where the red lines signify trajectories for pathway A_1B_1 with a pattern assumed at steady-state.

3 Kinematic models

3.1 Global theory

Consider a unit mass of a tracer (either active or passive) that is injected over a recharge area A where A denotes both a location of finite size (from which multiple trajectories emerge) as well as the localized area itself [L^2] at $t = 0$ as a pulse (red streamlines in Fig. 1). From the injection location $\mathbf{a} \in A$, a tracer particle follows a trajectory along a steady-state flow pattern (i.e., the pathway form -including length- does not change with time) to a discharge location $\mathbf{b}$; the associated water particle travel time is $\tau(\mathbf{a}, \mathbf{b})$.

$\tau(\mathbf{a}, \mathbf{b})$ is a random variable, as a result of velocity variations due to flow heterogeneity on scales of aquifers within a catchment that will generally be of various size. Average water travel time of an ensemble of tracer particles injected over A from A to B (i.e., along a pathway AB) is computed as (Destouni & Graham, 1995)

$$T(A, B) = \frac{1}{A} \int_A \tau(\mathbf{a}, \mathbf{b})\, d\mathbf{a} \qquad (1)$$

The variability of $\tau(\mathbf{a}, \mathbf{b})$ between A and B is attributed to as *macro-dispersion*.

The impact of catchment morphology and boundary conditions that prevail under hydrological forcing is referred to as *morphological dispersion*. The variability of $T(A, B)$ (equivalent to the mean of τ along a pathway as given in (1)) is attributed to morphological dispersion, quantifying differences between $T(A_1, B_1)$, $T(A_2, B_2)$, etc (Fig. 1).

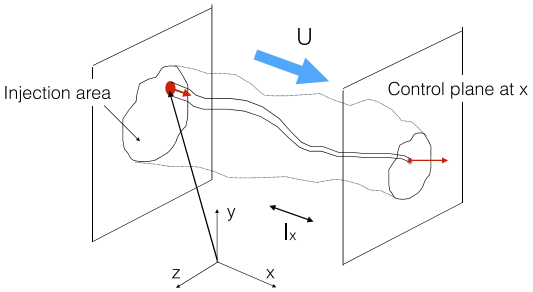

Figure 2: Configuration sketch of the axial hydrodynamic transport along pathways with time dependent mean velocity $U(t)$.

The tracer mass flux or discharge at $\mathbf{b}$ is $J(t,\tau)$ [M/T/L^2]. If the tracer is discharged over B, the total mass discharged between A and B (Figure 1) up to time t is

$$m(t;\mathrm{A},\mathrm{B}) = \frac{1}{\mathrm{A}}\int_0^t \int_{\mathrm{A}}\int_{\mathrm{B}} J[t',\tau(\mathbf{a},\mathbf{b})]\, d\mathbf{b}d\mathbf{a}\, dt' \tag{2}$$

in which the injected tracer is assumed to be uniformly distributed over A. Note that $d\mathbf{a}$ and $d\mathbf{b}$ have dimensions [L^2]. Our assumption is that the variability of τ over A (macro-dispersion) can be described by a probability density function (PDF) of τ conditioned on the mean T, denoted as $f(\tau \mid T)$. Then the tracer mass discharged from B (2) can be written as

$$m(t;\mathrm{A},\mathrm{B}) \approx m(t \mid T) = \int_0^\infty J(t,\,\tau)\, f(\tau \mid T)\, d\tau \tag{3}$$

3.2 The kinematic pathway model

3.2.1 *Hydrodynamic transport along a single pathway*

Consider transport of a tracer originating at A ($x = 0$) at t_0 along a single hydrological pathway AB under unidirectional transient flow, discharging at B, ($x = L$), at time $t = T$ with the time varying mean velocity of $U(t) = U_0\,\phi(t)$, in which $\phi(t)$ is an arbitrary dimensionless temporal function, and U_0 [L/T] a constant (Fig. 2). A simplified analytical model for water travel time cumulative distribution function (CDF) under arbitrary transient flow, along one-dimensional hydrological pathways with mean flow approximately uniform in space and constant macro-dispersivity is then (Paper I)

$$F_{AB}(t;x) = \frac{1}{2}\mathrm{erfc}\left[\frac{x - U_0\Phi(t)}{\sqrt{4\alpha_L U_0\Phi(t)}}\right] \tag{4}$$

where

$$\Phi(t) \equiv \int_{t_0}^{t} \phi(t')\,\mathrm{d}t'$$

Similarly, the water age CDF is derived using an inverted temporal variability function ϕ_b, defined as $\phi_b(t) \equiv \phi(T - t)$, whereby the mean flow velocity for the backward computation becomes (Paper I).

$$F_{BA}(t;x,\theta) = \frac{1}{2}\,\mathrm{erfc}\left[\frac{x - U_0\Phi_b(t,\theta)}{\sqrt{4\alpha_L U_0\Phi_b(t,\theta)}}\right] \tag{5}$$

where

$$\Phi_b(t,T) \equiv \int_0^t \phi_b(t')dt' = \int_0^t \phi(T-t')\,dt' \tag{6}$$

and α_L is the axial macro-dispersivity; for simplicity the initial time has been set to zero.

3.2.2 *Hydrodynamic transport along catchment pathways*

Consider a catchment of length scale L; a configuration sketch is given in Fig. 3a. The net precipitation (precipitation minus evapotranspiration) $P_n(t)$ [L^3/T] is an input function of time, and the flow discharge from the catchment is an associated output function of time $Q(t)$ [L^3/T]; the groundwater storage also changes in time. The most basic kinematic quantity for the waterborne tracer transport through a catchment follows from the fact that there is one preferred direction of the transport along each pathway, from the upstream input point (A_i) to the downstream location of entrance into the stream network (B_i) and then further to the catchment outlet (Fig. 1). To apply $U(t)$ (defined as the mean transient velocity along a single pathway in the previous section Fig. 2) to over and through all of the catchment pathways, as an overall kinematic measure of transport, over the scale L, $\phi(t)$ and U_0 need to be estimated for the overall catchment scale. The latter is summarized in section 3.2.3.

Conceptualization

For each unit of tracer mass entering the catchment system at any point, a flow trajectory can

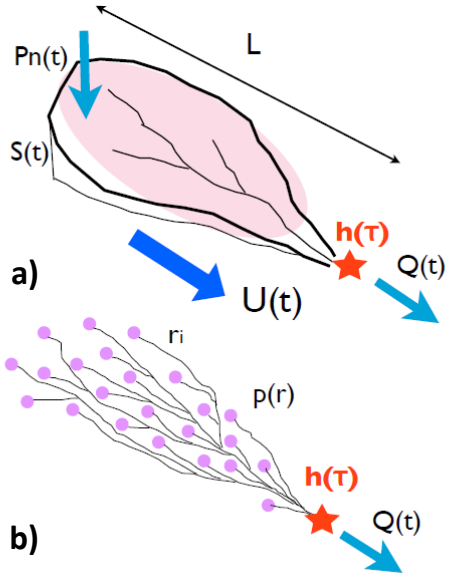

Figure 3: Configuration sketch of a) catchment of scale L with a net precipitation rate $P_n(t)$, flow discharge $Q(t)$ and catchment mean velocity $U(t)$, where $f(\tau)$ is the catchments scale travel time distribution; b) pathways from different recharge locations to discharge locations, with lengths $0 < r < L$ with a PDF $p(r)$.

be defined from elementary source locations to the discharge outlet of any considered catchment (Fig. 3b). A tracer follows a flow path (or transport pathway) with length r through different hydrological subsystems of the catchment (soil water, groundwater, stream). Although there are exceptions depending on topography and morphology, the water input $P_n(t)$ constitutes a driving force for the water flow through the catchment, from the land surface to the discharge outlet location over the characteristic catchment length scale L, along the main flow direction through the catchment.

To conceptualize the hydrodynamic transport through a catchment, a set of pathways from a corresponding set of elementary source input locations (locations A_i in Fig. 1), through subsurface water and into the surface water network (at locations B_i in Fig. 1), and further through the latter to the catchment outlet, is considered. Pathways to the outlet will thereby be of different length r_i (for pathway i), and also along each pathway a tracer will be dispersed longitudinally due to variations between different tracer trajectories prevailing within the elementary volume of each pathway i (red thin lines in Fig. 1). Aggregating all pathways over the whole catchment to the outlet, we capture transport through the entire catchment.

3.2.3 The kinematic pathway approach

To capture hydrodynamic transport through a catchment under transient unidirectional flow condition, the KPA is developed based on the analytical model for axial transport along a single pathway (4) and (5) with a link to the catchment structure and boundary condition as follows:

- The flow is transient only in magnitude but the overall flow pattern is temporally stable; the flow pattern is quantified by a pathway length PDF $p(r)$ [1/L] where r is inferred from topography in some suitable manner.
- The aquifer system of any catchment consists of aquifers that are essentially independent, relatively small and shallow; the depth of the aquifer system of any catchment is available as an average (or effective) aquifer thickness $\bar{h}$ [L] for the entire catchment or parts of the catchment.
- The basic driver of tracer transport is $U(t)$ (as expressed in (4) and (5)) for the entire catchment; where $\phi(t)$ is a temporal variability function inferred here from the transient behavior of the normalized $Q(t)$; the key kinematic driver for the analysis, catchment characteristic velocity U_0 [L/T] is inferred from the overall water balance using $\bar{h}$, $P_n(t)$ and L.

Given (4) and (5) for an arbitrary pathway AB of length r_i, tracer transport over the entire catchment is obtained by aggregation using $p(r)$ as (Paper II)

$$F_f(t;L) = \frac{1}{L}\int_0^L p(\xi) F_{AB}(t;L,\xi)d\xi \qquad (7)$$

which is the CDF of the water travel time given as a function of $p(r)$. Similarly, the CDF of the water age is

$$F_b(t;L,\theta) = \frac{1}{L}\int_0^L p(\xi) F_{BA}(t;L,\theta,\xi)d\xi \quad (8)$$

In (7) and (8), $p(r)$ will be inferred from topographical data, where a finite number of r_is will be considered. For simplicity of notation, we shall use $p(r_i)$ to signify the discrete distribution.

The catchment characteristic velocity

The characteristic velocity of the catchment $\bar{U}_0$ is estimated by the scale of the catchment L, the mean depth of the aquifer from the underlying bedrock layer or mean measured aquifer thickness $\bar{h}$, as

$$\bar{U}_0 = \frac{L \times (\bar{P} - \overline{ET})}{\bar{h}} \equiv \frac{L \times \bar{P}_n}{\bar{h}} \qquad (9)$$

where, $\bar{P}$ and $\overline{ET}$ [L/T] are the annual long-term average precipitation and actual evapotranspiration, respectively. The $\overline{ET}$ can be obtained from an empirical formula suggested by (Meinardi *et al.*, 1995) using $\bar{P}$ and long term average annual potential evapotarnspiration ($\overline{PET}$), for which $\overline{PET}$ is calculated from long term average annual temperature.

Dispersion

Catchment-scale dispersion is a results of two processes: morphological dispersion (attributed to the variability of pathways lengths from recharge to discharge locations), and macro-dispersion (attributed to the heterogeneity in hydraulic properties within pathways); morphological dispersion will depend on inferred $p(r)$, whereas macro-dispersion will be assumed Fickian with a specified Péclet number (Pe).

Morphological dispersion

The catchment system is considered here to be composed of stream channel, overland and shallow groundwater compartments. The $p(r)$ for associated pathways of each compartment with different length r_i, reffed to as $p(r_i)$ is extracted. In a shallow groundwater the length of any local groundwater pathway discharging to the adjacent stream channel or lake at any point within the catchment, is a function of the topographical distance of elementary source location to the outlet point following the local slope along the pathway (Goderniaux *et al.*, 2013). Hence, overland and shallow groundwater compartments are merged into one compartment for which the pathways are referred to as hillslope pathways. To study the impact of morphological dispersion, three possible scenarios of $p(r_i)$ for the catchment system are considered; these are referred to as:

case a: lumped pathway length distribution

case b: hillslope pathway length distribution

case c: hillslope/channel pathway length distribution

For case a, we consider only one single lumped compartment together for hillslope and channel flow in which any particle entering into the system at any point/cell takes the longest flow path available to the catchment outlet following the local slope without the possibility of discharging into the adjacent stream channel or lake along the way.

The ensemble of lengths extracted for case b is the distance along the flow path for each particle until it reaches the main river where it is transported to the downstream outlet point instantaneously (Darracq *et al.*, 2010). To delineate hillslope/channel separation, the critical drainage area of actual channel heads is obtained by defining a drainage capacity parameter denoted by c_{drain} , as the area contributing to runoff which localizes channel head locations (assumed to appear gradual and as a result of saturation of overland flow). To manually calibrate the c_{drain} parameter, localized head locations are latter compared to the river network field data.

Case c $p(r_i)$ is obtained in a similar manner as in case b for hillslope pathway lengths, plus pathways corresponding to channel flow compartment. As for stream channel cells, the ensemble of pathway lengths is calculated as the topography-driven downstream distance c_{drain} along the stream for each cell.

Macro-dispersion

Macro-dispersion can be quantified by specifying Pe defined by

$$\mathrm{Pe} = \frac{2}{\zeta_0^2} \quad ; \quad \zeta_0 = \sqrt{\frac{2\,\alpha_L}{r}} \quad ; \quad \alpha_L = \frac{r}{\mathrm{Pe}} \qquad (10)$$

where ζ_0 is the coefficient of variation (CV) for tracer travel time along trajectories, τ. Hence, by fixing Pe for a catchment, α_L becomes a function of the pathway scale, r, as defined in (10).

Tracer discharge

The discharge of a passive tracer (mass per unit time) at the outlet of a catchment under transient flow conditions, is quantified as a hydrodynamic transport measure. Tracer discharge at a catchment outlet is a time series that is described by a statistical distribution and a correlation structure, with emphasis on the value range (percentiles).

First, the tracer input over the entire catchment surface per unit catchment area, J_0 [M/T/L^2] is obtained using $P_n(t)$ with two levels of resolution (daily, and monthly), and $C_0(t)$ [M/L^3], a temporal series of input tracer concentration (i.e., from atmospheric deposition). Typically, $J_0(t)$ and the tracer discharge per unit catchment area at the outlet location $J(t)$ exhibit random temporal variations, where J is predominantly determined by J_0 weighted by the travel time PDF (or frequency function) (Niemi, 1977; Rodhe *et al.*, 1996; Kirchner *et al.*, 2000). This is computed by a convolution

$$J(t;x) = \int_0^t J_0(t-\theta)\, f(\theta;L)\, d\theta \qquad (11)$$

where $f(T)$ [1/T] is the travel time PDF (or frequency function) of T (1), given by (7). The L in (11) signifies the catchment outlet location, for which the PDF $f(T)$ is computed. Note that α_L in (4) is defined by (10), i.e., it depends on r for a fixed Pe.

The KPA can now be summarized as follows. Given the input information $P_n(t)$, $C_0(t)$, $Q(t)$ and $\bar{h}$, as well as the geographical-topological definition of a catchment, we compute $J(t)$ using (11), where $f(T)$ is obtained from (7) using (4) with specified Pe. The input $J_0(t)$ is computed from $C_0(t)$ and $P_n(t)$, whereas the key kinematic quantity for the analysis, U_0, is inferred from tracer and water mass balance, $\phi(t)$.

3.3 Retention and transformation

3.3.1 Hydrodynamic transport model

The most general analytical form of the water travel time PDF, f, for hydrodynamic transport as TOSS density (Cvetkovic, 2011a) is defined in the Laplace Transform (LT) domain as

$$\widehat{f}(s) = \exp\left[ca^\alpha - c(a+s)^\alpha\right] \qquad (12)$$

where $0 \le \alpha \le 1$ and $a, c > 0$. The parameters a, c and α are related to $\overline{\tau}$ and ζ_0, respectively, as

$$a = \frac{1-\alpha}{\overline{\tau}\zeta_0^2} \quad ; \quad c = \frac{\overline{\tau}}{\alpha a^{\alpha-1}} \qquad (13)$$

For $\alpha = 1/2$, the TOSS density is a solution of the advection-dispersion equation with injection and detection in the flux (i.e., the inverse-gaussian distribution), with parameters a and c defined by

$$a = \frac{U}{4\alpha_L} \quad ; \quad c = \frac{x}{\sqrt{\alpha_L\, U}} \qquad (14)$$

where U is the mean velocity and α_L the dispersivity, whereby $\zeta_0 = \sqrt{2\alpha_L/x}$.

3.3.2 Mass transfer model

A general form of the partition function $g(t)$ has been presented using a Pareto multi-rate distribution, suitable for capturing Fickian as well as non-Fickian diffusive mass transfer combined with sorption (Cvetkovic *et al.*, 2016):

$$\begin{aligned} &\widehat{g}(s) = A \cdot {}_2F_1\left(1, \nu, \nu+1, -s/k_0\right) \quad ; \\ &g(t) = A\,\nu k_0\, E_\nu(tk_0) \end{aligned} \qquad (15)$$

where ${}_2F_1(\cdot)$ is the hypergeometric function, $E(\cdot)$ the exponential integral function and A is the partitioning (sorption) coefficient once equilibrium is reached. For an arbitrary exponent ν, g (15) is a partition function for a generalized (non-Fickian) diffusive mass transfer model. The special case with $\nu = 1/2$ is applicable for Fickian diffusive mass transfer.

Mass attenuation

An attenuation index η is an order-of magnitude count of the mass ultimately discharged between *A* and *B* obtained as

$$\eta(T) = -\ln\left\{\widehat{f}\left[\lambda\left(1+\widehat{g}(\lambda)\right) \mid T\right]\right\} \qquad (16)$$

Equation (16) is valid in the case decay takes place in both mobile and immobile phases with the same, uniform rate λ [1/T]. Special case of decay (or degradation) in the aqueous phase only, is obtained by setting mass transfer to zero, i.e., $g = 0$; then we have

$$\eta(\tau) = -\ln\left[\widehat{f}\left(\lambda \mid T\right)\right] \qquad (17)$$

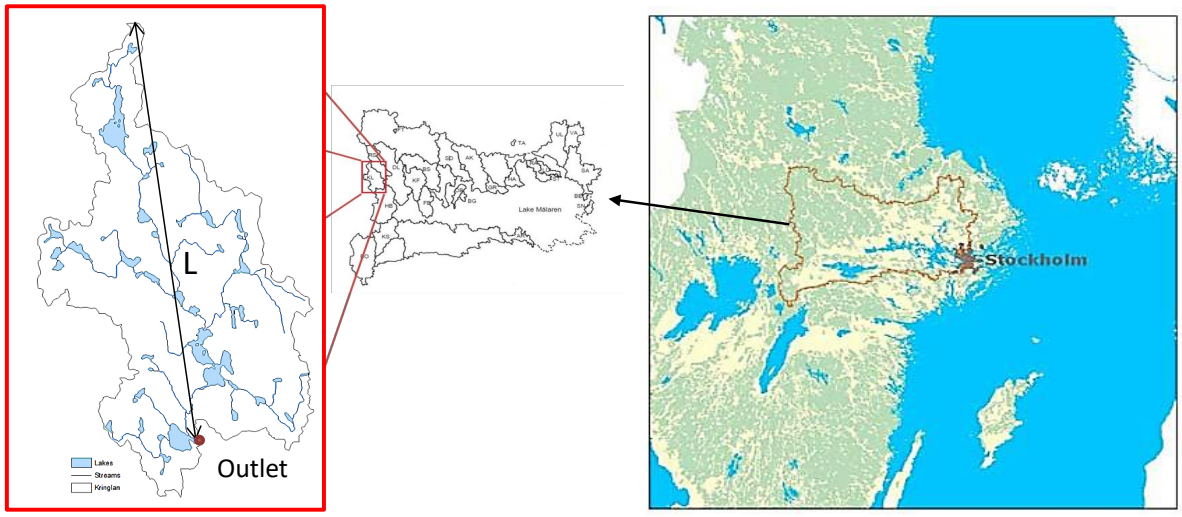

Figure 4: Case study I: Kringlan catchment is located in east-middle Sweden, on the western boundary of the Norrström drainage basin adapted from (Xu, 2003). The catchment has an area of 294.5 ***km***^{2} ***and a scale of*** $L = 30.43$ ***km as the longest distance length to the outlet.***

Using (16) or (17), NAP can be computed as

$$\mathrm{CCDF}(\eta) = \mathrm{CCDF}_T[T(\eta)] \qquad (18)$$

where CCDF_T is the complementary CDF (CCDF) of T. The $\mathrm{CCDF}(\eta)$ can be computed directly using the ensemble of T. The variations of T can be assumed (or inferred) by the general kinematic model, quantified by the kinematic pathway model or numerically simulated using a dynamic model.

4 The dynamic model

Numerical simulations of surface and groundwater flow as an integrated hydrological system (with surface/subsurface flow interactions), and the associated advective transport, is performed by means of the state-of-the-art tool MIKE SHE (Graham & Butts, 2005; Butts & Graham, 2005).

Numerical computation of T distributions is carried out by running the Random Walk particle tracking module available in MIKE SHE water quality package, where pure advection is considered. One passive particle per each recharge cell with the general notation of such a cell A is instantaneously released from the first layer of the saturated groundwater zone into the groundwater system. Note that the particles are only traceable as long as they are in the groundwater (saturated zone). Flow paths of particles moving from source locations in saturated zone to different discharge locations with the general notation of such locations B, e.g. rivers, drains, the unsaturated and overland flow zones are simulated.

RESULTS

This section summarizes the principal results examined in view of the thesis objectives. The appended journal publications (Paper II and Paper IV) provide additional details relevant to the main theme of each paper. The focus is on the two case studies of tracer discharge characteristics that form the bases of the thesis. The applications of the proposed models (kinematic pathway and dynamic coupled with retention and transformation) are illustrated through the case studies that represent two actual catchments in Sweden.

5 Case study I

Case I quantifies the statistical distribution of continuous tracer discharge from a boreal catchment under transient flow using the *kinematic pathway model*. The model is applied to estimate a 23-year long chloride data series dis-

charge for the boreal catchment of Kringlan located in east-middle Sweden, on the western boundary of the Norrström drainage basin (Fig. 4). The Norrström basin is situated on the east coast of Sweden with the outlet located in Stockholm, discharging into the Baltic Sea (Fig. 4).

5.1 Model setup

To compute $J(t)$ at the Kringlan catchment outlet location using (11), $f(T)$ and $J_0(t)$ are the model inputs; $f(T)$ is obtained from (7) using (4), whereas input $J_0(t)$ is estimated from $C_0(t)$ and $P_n(t)$ data series retrieved from Swedish University of Agricultural Sciences database (SLU, 2012) and Swedish Meteorological Hydrology Institute (SMHI, 2012), respectively, as $J_0(t) = C_0(t)P_n(t)$. The $P_n(t)$ data series are available daily (Fig. 5a) and monthly (Fig. 5b), whereas only monthly values are available for $C_0(t)$ time series.

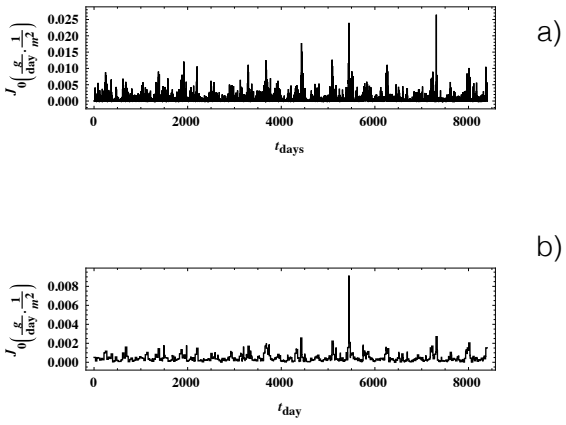

Figure 5: Measured chloride input discharge $J_0(t)$ obtained from the measured concentration $C_0(t)$ and net precipitation $P_n(t)$ for the Kringlan catchment as $J_0(t) = C_0(t)P_n(t)$. We shall use two temporal resolutions for J_0: a) daily J_0, obtained with daily $P_n(t)$ and monthly $C_0(t)$; b) monthly $J_0(t)$, obtained using monthly $P_n(t)$ (computed by averaging daily $P_n(t)$) and monthly $C_n(t)$. Note that only monthly data is available for the chloride concentration in the precipitation, $C_0(t)$.

5.1.1 Water travel time distribution

The input parameter values summarized in Table 1, and also input functions of $\phi(t)$ and $p(r_i)$ as illustrated in Fig. 6 and Fig. 7, respectively, are used to calculate $f(T)$ for the whole Kringlan catchment.

Table 1: The input parameter with their corresponding values used in KPA for tracer discharge quantifications from Kringlan catchment .

parameter	value	unit	source
L	30.43	km	(Lantmäteriet, 2012)
U_0	5.72	m/day	eq. (9)*
Pe	20	[ ]	assumption
c_{drain}	1	km^2	(SMHI, 2012)**

Note: *h in (9) is considered the mean depth to the bedrock; data retrieved from Swedish Geological Survey (SGU, 2016).**The c_{drain} is obtained in terms of number cells (=400) in comparison to rivers and lakes data, retrieved from (SMHI, 2012).

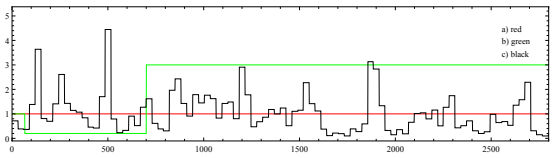

Figure 6: Sample dimensionless temporal function $\phi(t)$ (black lines) considered in computations of water travel time CDF: obtained from the normalized monthly averaged discharge measurements showed for 2800 days at the outlet of the Kringlan catchment (Sweden).

Input function of $\phi(t)$ is inferred from the transient behavior of the normalized $Q(t)$ at the outlet of the Kringlan catchment, data series obtained from (SMHI, 2012). Fig. 6 shows a 2800 days sample of $\phi(t)$ time series as the black line. The three potential $p(r_i)$ cases of **a-c** as summarized in section 3.2.3, for the catchment system are extracted from $50m \times 50m$ resolution DEM data (Lantmäteriet, 2012) using 'Flow length tool' of Arcmap 10.4. One can see in Fig. 7a, the pathway lengths are randomly distributed over a range between 0 and 36km (i.e., $0 < r_i < 36$km). As for case **b** the drainage capacity (c_{drain}) of 400 cells obtained from the river network data is used as the weighting raster for the 'Flow length tool'. The $p(r_i)$ for case **b** shows features of a semi-gamma distribution with emphasis on shorter distances (Fig. 7b). Similar to case **b**, $p(r_i)$ for case **c** shows features of a semi-gamma distribution, again emphasizing shorter distances; however, case **c** spans over a wider pathway length range, with a longer tail (Figure 7c).

Fig. 8 shows the TTD calculated at the Kringlan

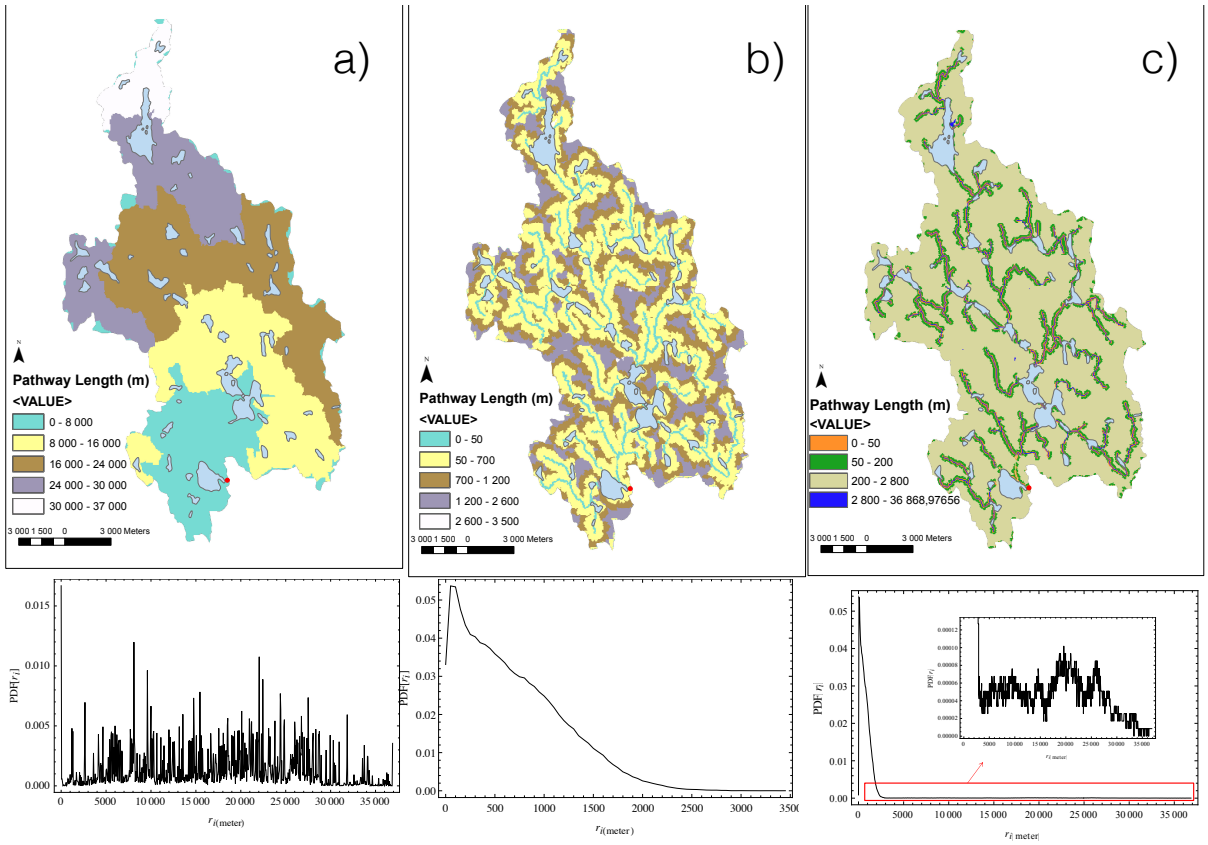

Figure 7: Three potential pathway length distributions $p(r_i)$ for the Kringlan catchment: a) lumped pathway length distribution, b) hillslope pathway length distribution, and c) hillslope/channel pathway length distribution.

catchment outlet with different morphological dispersion scenarios of case **a** (lumped $p(r_i)$, green curve), case **b** (hillslope $p(r_i)$, cyan curve) and case **c** (hillslpe/channel $p(r_i)$, red). Case b (cyan curve) with dominance of shorter lengths, exhibits the fastest transport up to 4 years (Fig. 8) which aims to represent hillslope flow, basically the fast response of the catchment in the event-scale of a year. Finally, case **c** travel time distribution (green curve) which targets transport through both hillslope and stream channel flow paths, resides in between cases **a** and **b**. The alternative water TTDs as summarized in Fig. 8 are then used as the input functions for tracer discharge distribution quantifications.

5.2 Model output

The basic data used are 23 years (1985-2008) of chloride monthly concentration time series available both in the rainfall and outlet of the Kringaln catchment (SLU, 2012). Combining the chloride concentration and water discharge data at the outlet, we computed the measured (observed) chloride discharge denoted as $\bar{J}$, from which a distribution was extracted as CDF($\bar{J}$).

Fig. 9 shows the computed/estimated CDF(J) (solid lines) and CCDF(J) obtained using (11), and compares these to the observed CDF($\bar{J}$) and CCDF($\bar{J}$) for the Kringlan catchment, shown on a logarithmic scale. The CDF(J) and CCDF(J) are shown for different scenarios of water travel time PDF computation, i.e., cases **a**, **b** and **c**.

The overall representation of the CDF(J) and CCDF(J) for chloride by the models is poor when monthly input $J_0(t)$ is used (Figure 9a) improving for input based on daily measurements (Fig. 9b). The comparison can be further elucidated by considering maximum, minimum discharge values, as well as different percentiles (5, 50 and 95), that are summarized

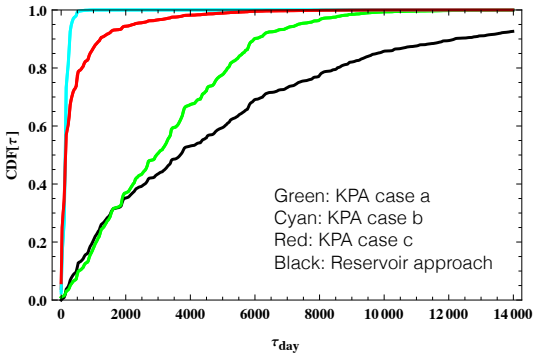

Figure 8: Kringlan catchment travel time distributions calculated using the KPA for different cases: a) lumped (green), b) hillslope (cyan), and c) hillslope/channel (red) pathway length distribution.

Table 2: Statistical measures of the chloride discharge distribution. Measured values are compared to model output obtained using the KPA for three cases of $p(r)$ estimation: case a (lumped), case b (hillslope), and case c (hillslope/channel). Both the measured $\bar{J}(t) = C(t)Q(t)$ and modeled $J(t)$ with input $J_0(t) = P_n(t)C_0(t)$ use monthly averaged values of $P_n(t)$ and $Q(t)$. The period is 1985-2008.

	measured	case a	case b	case c
max	0.0024	0.0006	0.0012	0.0012
min	0.00003	0.00038	0.00017	0.00026
5 %	0.00008	0.00041	0.00026	0.00031
50 %	0.00041	0.00047	0.00043	0.00043
95 %	0.00135	0.00054	0.00086	0.00071

All values are in $(g/day.1/m^2)$.

in Table 2 for monthly data and Table 3 for daily data. It follows from Tables 2 and 3 that the 50-percentile is in fact best represented by the monthly data, whereas the extreme values (high and low) are better represented by the daily data. Specifically, the maximum, the minimum, 5 and 95 percentiles for case **b** are most consistent with measured data (Table 3); the 50 percentile for case **c** with stronger morphological dispersive features, compares best with data. Generally, the highly random $p(r_i)$ case **a** does not capture the high values of tracer discharge, which is reflected by entries in Tables 2 and 3.

Among all considered cases with different morphological dispersion, the case **b** with relatively fast responses up to approximately four years, yields estimates that compare closest to the measured chloride discharge distribution. In a

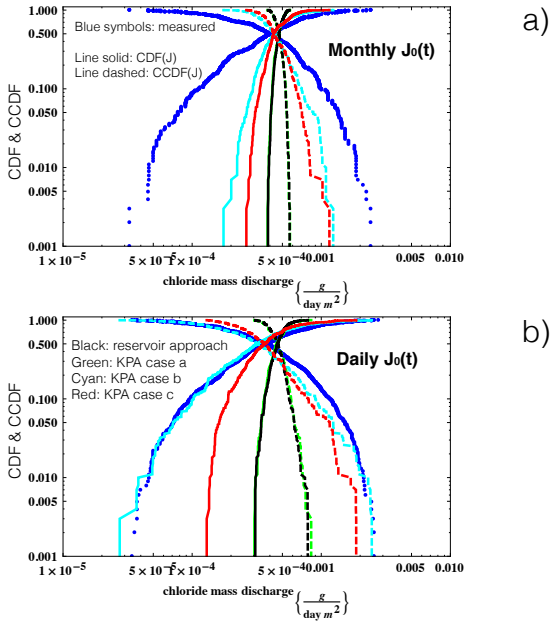

Figure 9: Estimated CDFs (solid) and CCDFs (dashed) of chloride mass discharge from Kringlan catchment are compared to measured data, presented on a logarithmic scale. Chloride discharge values are in [g/day/m^2] and have been calculated using: a) monthly $J_0(t)$; b) daily $J_0(t)$. The CDF(J) and CCDF(J) obtained using KPA with three different $p(r)$, are compared to measured CDF($\bar{J}$) and CCDF($\bar{J}$); the CDF(J) and CCDF(J) obtained using the reservoir (or reactor) approach is also included. Pe in these calculations is 20.

Table 3: Statistical measures of the chloride discharge distribution. Measured values are compared to model output obtained using the KPA for three cases of $p(r)$ estimation: case a (lumped), case b (hillslope), and case c (hillslope/channel). Both the measured $\bar{J}(t) = C(t)Q(t)$ and modelled $J(t)$ with input $J_0(t) = P_n(t)C_0(t)$ use daily values of $P_n(t)$ and $Q(t)$. The period is 1985-2008.

	measured	case **a**	case **b**	case **c**
max	0.0028	0.00084	0.0025	0.0019
min	0.00003	0.00064	0.00003	0.00013
5 %	0.00007	0.00034	0.00007	0.00016
50 %	0.00038	0.00045	0.00032	0.00037
95 %	0.0015	0.0006	0.0012	0.0012

All values are in $(g/day.1/m^2)$.

catchment system with shallow and independent aquifers, the transport is strongly influenced by hillslope processes i.e. surface and subsurface runoff; in such systems, the contribu-

tion of deeper groundwater to the catchment-scale transport is comparatively small, the water predominantly being flushed away on an event-scale.

6 Case study II

The distribution of decaying tracer discharge from a well characterized boreal catchment under steady-state flow with focus on long-term transport ($\approx$ 400 years) is quantified using the integrated dynamic model in comparison to kinematic pathway model estimates. The model is applied to estimate NAP (see section 3.3.2) as the measure for active tracer discharge for the coastal catchment of Forsmark, with an area of 180 km^2 located in eastern Sweden where it borders the Baltic Sea (Fig. 10).

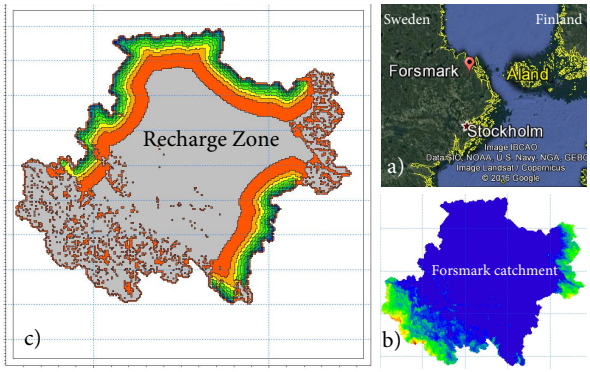

Figure 10: Case study II: a) Forsmark location, b) model domain (sea levels are in blue where other colors represent topographical values above the sea level), c) recharge zone is in gray where other colors show discharge zones with respect to the discharge rate magnitude.

6.1 Model setup

To determine NAP as the CCDF(η) for the entire system, using (18) with (17) together with the TOSS density (12), $f(T)$ is quantified from particle tracking MIKE SHE simulations for the entire catchment. The parameters a and c of TOSS density are then obtained in terms of mean travel time in (13) where T replaces $\bar{\tau}$ and $\alpha = 1/2$ and ζ_0 are considered to implement Fickian transport with axial macro-dispersion along the pathways. Model parameters are summarized in Table 4.

Table 4: The input parameters with their corresponding values used for active tracer discharge quantifications from the Forsmark catchment.

parameter	value	unit	source
α	$\frac{1}{2}$	[ ]	assumed
λ	0.001	1/day	assumed
ζ_0	0.1, 0.3	[ ]	assumed
$\overline{T}_{SIM}$	7667	days	dynamic model
$\overline{T}_{EST}$	9210	days	$\bar{h}/(\bar{P}-\bar{ET})$*
ζ_{SIM}	2.3	[ ]	dynamic model
ζ_{EST}	1.35, 3	[ ]	kinematic pathway method
c_{drain}	0.5	km^2	(SMHI, 2012)**

Note: *$\bar{h}$ = 3.5 m and $\bar{P}-\bar{ET}$ =0.38 mm/day; data obtained from SGU (2016) and SMHI (2012), respectively.**The c_{drain} is obtained in terms of number cells (=80) in comparison to rivers and lakes data, retrieved from SMHI (2012).

6.1.1 *Water travel time distribution*

Numerical simulation of T distribution for 375 years of temporally stable recycled flow field, with one passive particle per cell released over the entire recharge zone (Fig. 10c) is presented in Fig. 11 as the orange histogram. The relative effects of morphological and macro-dispersion on $f(T)$ are illustrated. The orange histogram shows the PDF of travel time assuming only morphological dispersion, that is, without any macro-dispersion. The three curves in Fig. 11 combine morphological and macro-dispersion of different degree, from the blue curve as the lowest, and the red curve as the highest. Fig. 11a & b show the same cases, but the time range considered is different, and similar for Fig. 11c & d. Comparing curves of same color in Fig. 11a & c, one can see that the histograms are relatively close, although the deviation is visible for larger macro-dispersion (red curve); this difference cannot be seen in the tail part of the breakthrough curve (BTC). A closer look at the initial part of the BTC in Fig. 11b & d, reveals that the blue and green curves are indeed very close, whereas the red curves in Fig. 11b & d do not significantly differ. The results presented in Fig. 11 confirm that two representations of the macro-dispersion with constant Peclet number and constant dispersivity, respectively, yield results that are indistinguishable for all practical purposes.

6.2 Model output

Having characterized the T distribution along pathways (with assumed ζ_0) for all particles al-

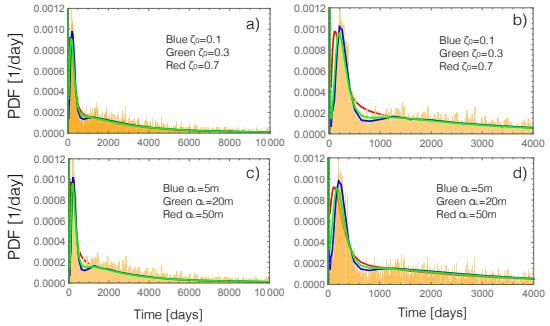

Figure 11: The probability density functions (PDFs) of Forsmark catchment water travel time with (lines) and without (orange histogram) macro-dispersion: a) & b) assuming a fixed coefficient of variation ζ_0 of travel time; c) & d) assuming three fixed values of the macrodispersivity α_L. The data in b) and d) are identical to those in a) and c), respectively, but the time range shown is smaller.

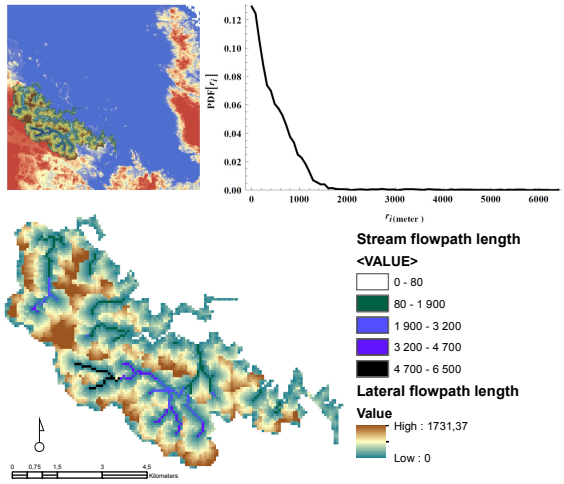

Figure 12: Hillslope/channel flow path lengths distribution for western land portion of the Forsmark catchment. The pathway length distribution $p(r_i)$ spans over 0 to 6500 meters with the emphasis on shorter distances.

lows computations of NAP through the Forsmark catchment, with the assumption of morphological dispersion governed by an inverse-gaussian distribution, with mean $\bar{T}$ and CV of T, $\zeta = \sqrt{\mathrm{Var}(T)}/\bar{T}$. Two sets of values are used for $\bar{T}$ and ζ, one obtained from MIKE SHE numerical simulations and the other estimated from basic hydrological and structural/geometrical information as summarized in Table 4. $\bar{T}_{EST}$ is estimated as the CV of r ensemble extracted using the pathway method (as explained under section 5.1.1) and shown in Fig. 12. The CCDF of η (or NAP) is illustrated in Fig. 13 with the dashed red and blue lines, assuming macro-dispersion as low $\zeta_0 = 0.1$ (blue dashed line) and high $\zeta_0 = 0.3$ (red dashed line). The estimate of the simulated NAP (symbols) is poor because the morphological dispersion is underestimated (compare simulated CV of 2.3 with its estimate of 1.35, Figure 13).

To improve the morphological CV estimate and in view of the skewness of the pathway length distribution (Fig. 12), the median is used instead of the arithmetic mean to compute the geometrical pathway length CV; the obtained value is 3. Fig. 13 shows Forsmark NAP with ζ_{EST} as the solid blue line ($\zeta_0 = 0.1$) and solid red line ($\zeta_0 = 0.3$). The analytical estimate is now very close to the simulated CCDF(η), indicating that this may be an effective means to account for morphological dispersion.

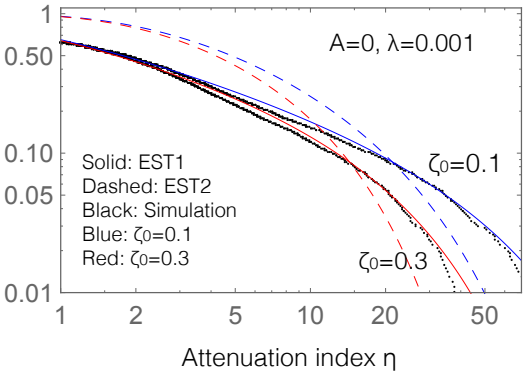

Figure 13: Comparison of simulated and analytically estimated Forsmark catchment NAP for different cases of macro-dispersion, and using different estimates of the coefficient of variation ζ that quantifies morphological dispersion. The coefficient of variation of T that quantifies morphological dispersion is 1.35 for case EST1 and 3 for EST2. A non-sorbing solute is used here for illustration. ζ_0 quantifies the macro-dispersion effect as the coefficient of variation of water travel time.

Discussion

To address the research question of applicability of broad kinematic pathway models for quantifying the tracer discharge, travel time and wa-

ter age distributions in hydrological transport, three key issues should be considered:

1. temporal scale;
2. spatial scale; and
3. data availability;

Temporal scale of the problem (i.e. day, season, year, decade or century) controls the type of solution, i.e. transient or steady-state. The choice of transient approach is inevitable when the dynamics of the system is characterized by short temporal scale. Temporal fluctuations of flow drivers at the event scale of a day, season or year induce changes in transport in a way that constrains the modeling approach to time variant solutions available in the kinematic pathway model suggested in this thesis, and also in dynamic models based on a resolved transient velocity field. However, steady-state kinematic (e.g. Haitjema, 1995) or dynamic (Goode, 1996; Varni & Carrera, 1998; Woolfenden & Ginn, 2009) models are the practical solutions for cases when the long-term impact of transport is important.

In large spatial scale modeling, spatial variations of transport are commonly neglected when using a fully mixed reservoir theory. However, the application of lumped parametric models with no capability of capturing spatially dependent transport processes, in some cases with respect to the objective of the analysis, may result inaccuracy. Alternatively, including some levels of spatial variability, for instance by using two-compartment models (Botter *et al.*, 2011) or KPA application, are valid options. However, the latter option only applies to catchments with shallow or topographically controlled groundwater flow systems.

The availability of tracer data series for commonly used kinematic models (Małoszewski & Zuber, 1982; Haitjema, 1995; Maloszewski & Zuber, 1996; Rodhe *et al.*, 1996; Kirchner *et al.*, 2000; McGuire & McDonnell, 2006; Kirchner *et al.*, 2001) and extensive field data (e.g. hydrological drivers and hydraulic properties) for dynamic models (Troldborg *et al.*, 2008; Fiori & Russo, 2008; Fiori *et al.*, 2009; Engdahl & Maxwell, 2015) are prerequisites. Whereas only basic hydrological and morphological information are needed for the kinematic pathway model application.

Catchment-scale hydrological transport is influenced by topography and can be partitioned between hillslope and larger regional scales (Goderniaux *et al.*, 2013). The simple kinematic pathway model for quantifying the travel time and water age distributions proposed in this thesis is only applicable for topographically-driven flow paths to adjacent discharge zones, e.g. rivers and lake through hillslope (shallow) compartments. Further studies on the extent to which topography influences flow path lengths and travel times in shallow hillslope compartments would help better understand the KPA applicability. The latter could be achieved through comparing dynamic models, with KPA computations for different shallow catchments. In conclusion, the thesis suggests a new approach for hydrological transport modeling in shallow catchments that avoids the need for detailed field data. The thesis has demonstrated the applicability of the proposed method to two selected catchments in Sweden.

7 Future perspectives of the kinematic pathway model

Potential developments of the kinematic pathway model could be done through increasing the accuracy levels of model parameter estimations. Furthermore, predictive capabilities of KPA for quantifying water age distributions at the catchment scale need to be evaluated and verified by environmental tracer data.

7.1 Characteristic velocity

The characteristic velocity (U_0) of the catchment is the overall kinematic driver of flow and transport. Considering a single mean velocity $\bar{U_0}$ using equation (9) to be representative for all flow compartments of channels, overland and shallow groundwater is a rough estimate. Alternatively, one can apply a water balance approach to quantify mean velocity for different flow compartments, using in/outflows of each compartment and its effective scale L_{eff}, e.g. $U_0 = Recharge \times L_{eff}/(\bar{h} \times n)$, where n is the mean porosity and $\bar{h}$ the average aquifer thickness, as an estimate of shallow groundwater mean velocity.

7.2 Morphological dispersion

A key challenge for accounting for morphological dispersion is inference of $p(r)$ based on topographical information. An alternative method for inferring the drainage capacity parameter (c_{drain}, see section 3.2.3), is to extract the critical drainage area from the traditionally used drainage area, slope log-log diagrams (Montgomery & Foufoula-Georgiou, 1993). However, the sensitivity of $p(r)$ to the c_{drain} parameter requires further investigation.

Recently, a study by Goderniaux *et al.* (2013) on groundwater partitioning shows that recharge fluxes are strongly influenced by topography and categorized between hillslope and regional scale. In fact, they suggest a two-compartmentalized TTD for a regional-scale catchment as

$$f(T) = \beta_1 \times f_1(T) + \beta_2 \times f_2(T) \qquad (19)$$

where, β_1 and β_2 are the proportion of "hillslope" and "regional" TTD, compartments. Moreover, $f_2(T)$ shows a mixed reactor behavior as an exponential function, whereas, $f_1(T)$ is a complex function with its shape controlled by local topography and the nested circulation structure close to the topography (the drainage capacity parameter; c_{drain}, of morphological dispersion in analogy with the KPA). The thesis results are qualitatively consistent with Goderniaux *et al.* (2013) results, but a new quantitative perceptive is suggested on "hillslope" travel times.

The concept of shallow (or hillslope) groundwater flow compartment applies only to highly permeable recharge zones adjacent to rivers or lakes. Here, it should be noted that no shallow aquifers exist in regions with dry channels. The c_{drain} which represents the hillslope area decreases with increasing recharge. Thus, the pathway lengths decrease which implies more emphasis on shorter distances and on transport dominated by morphological dispersion and fast response of the catchment. Consequently, studying the relationship betweens c_{drain} and recharge rates by comparing numerical simulations of travel time distributions with KPA computations for shallow catchments could reveal new insights into characterization of shallow aquifers.

An interesting perspective on recharge rates' control on transport (simulated T distribution) is obtained by comparing the CDF and CCDF of the Lagrangian and Eulerian velocities on the aquifer system scale in case study II (Figure 14). It is seen that the two distributions are very different. Whereas the Eulerian velocity spans a wide range of values, the Lagrangian velocity is dominated by most permeable subsurface regions in the catchment, and is thereby significantly shifted to higher values (Figure 14). Only a relatively small fraction of the velocities (<5%) contributes to the transport over the simulated 375 years. The Lagrangian velocity exhibits a power-law tail over a three-order of magnitude range with an exponent of approximately -4/3. It is interesting to note that the coefficient of variation of the Lagrangian velocity is around 3; it would be interesting to further explore the link between morphological dispersion and recharge zones with respect to their rates. Clearly more work is needed to better understand the relationship between recharge rates and topographical-driven flow under different conditions (including transient flow) and different heterogeneity conditions. Similar analysis have been done in generic studies of solute transport by groundwater (Cvetkovic *et al.*, 1996; Gotovac *et al.*, 2009). This observation

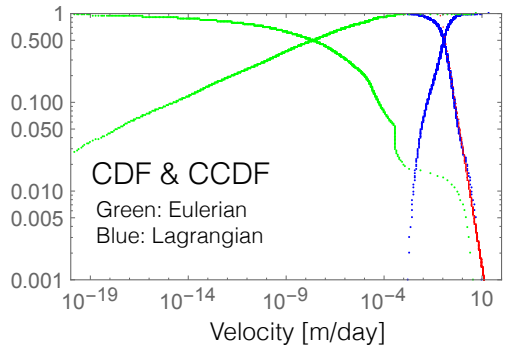

Figure 14: Cumulative and complementary cumulative distribution function of Lagrangian flow velocity extracted from MIKE-SHE particle tracking (blue), cumulative and complementary cumulative distribution function of Eulerian flow velocity extracted from numerical simulation MIKE-SHE (green) for the Forsmark catchment, Lagrangian velocity power-law tail over a three-order of magnitude range with an exponent of approximately -4/3 (red).

emphasizes two research questions of how to partition recharge zones into shallow (hillslope) and deep (regional) compartments, and how to extract proportion of each compartment. Answers to these questions enable application of simple yet physical transport models on regional scales for potential climatic impacts on transport, from simple contaminant classes of radionuclides, nutrients to complex class of priority organic pollutants. Moreover, such an approach can be used for assessing the overall catchment potential for self-purification that can be used for benchmarking nature-based solutions for the development of prevention and mitigation strategies.

7.3 Water age

Using eq.(8) for computing water age accounts for spatiotemporal variability of age distribution at catchment scale dominated by shallow aquifers. However, the proposed method in this thesis requires further evaluations and possible developments by application to real catchment case studies using deconvolution techniques (e.g. Engdahl & Maxwell, 2014) and environmental tracer data. This could broaden the applicability of the method to regional scales using basic hydrological and morphological information for evaluating potential future climatic impacts on groundwater resources from supply-demand management and planning point of view. Lastly, the presented pathway approach is applicable to the various types of time-dependent reactions (for which the groundwater age would be highly relevant) in principle on any spatial and temporal scales, e.g. individual recharge and discharge zones and for present (real) or future (hypothetical) temporal boundary conditions.

8 Summary and Conclusions

This thesis investigated the gap between kinematic and dynamic models for quantifying hydrological transport at catchment scale. Diverse measures of tracer discharge, travel time, age and natural attenuation potential were used to study hydrological transport governing mechanisms quantitatively. The main objectives were to develop a simple kinematic pathway model, apply it to real case studies and assess the predictive performance of the model in comparison with data. Moreover, an attempt was made to evaluate the impact of dispersion at different levels on transport considering various scenarios for macro and morphological dispersion. A framework for the kinematic pathway methodology was presented for estimating integrated hydrodynamic transport and mass transformation in its simplest form of linear decay/degradation. The latter was compared with simulations from a combined analytical and numerical model for a real catchment case study with steady-state flow. The following specific conclusions are drawn from the thesis:

1. A simple kinematic model for travel time and water age distribution were obtained in the form of eq.(4) and eq.(5) for a hydrological pathway defined in one spatial dimension along a mean flow. The proposed kinematic model is applicable for arbitrary time variations of the mean velocity and for axial macro-dispersion (Paper I);

2. The proposed travel time and water age distributions (Paper I) were extended to eq.(7) and eq.(8) and linked to the catchment structure and boundary condition for quantifying catchment-scale hydrological transport (Paper II);

3. A kinematic pathway approach (KPA) for computing tracer discharge per unit area [$M/T/L^2$] at the discharge point of a shallow catchment with a predominantly unidirectional mean flow following the topographical slope using equation (7) with (11) was developed (Paper II);

4. The predictive performance of kinematic pathway model was evaluated by application to a real catchment case study with chloride tracer data time-series considering three various morphological dispersion scenarios. The statistical distribution of tracer discharge obtained using the pathway length distribution that sufficiently skewed toward short pathway lengths, or short travel times compared closest to the measured chloride discharge distribution (Paper II).

5. The attenuation index as a measure of integrated hydrodynamic transport and mass transformation processes in the form of the

general distribution for hydrological transport (tempered one-sided stable density, TOSS) was presented. Macro-dispersion was found to be the most sensitive process of hydrodynamic transport in a single aquifer system with notable effect on attenuation (Paper III).

6. The framework for computing the natural attenuation potential of a catchment using eq.(18) with eq.(16) or (17) was introduced. The computation of travel times for a well-characterized shallow catchment case study under steady-state flow condition with focus on long-term transport was carried out by MIKE SHE and combined with the general distribution (TOSS) for macro-dispersion eq.(12). The dispersion process exerted the most influence on the travel time variations at two levels morphological and macro-dispersion. The simple kinematic pathway estimations of natural attenuation potential of the case study compared reasonably well with the dynamic model simulations (Paper IV).

The simple kinematic pathway model for quantifying hydrological transport proposed in this thesis is limited to topographically-driven flow paths to adjacent discharge zones, e.g. rivers and lake through hillslope (shallow) compartments. In other words, the proposed kinematic pathway approach is based on the controlling impact of topography on flow path length and travel time distributions in shallow catchments. Our work has shown that the pathway (Lagrangian) methodologies are promising as predictive tools for hydrological transport. Further comparison between kinematic and dynamic models is needed however to more accurately capture the role of subsurface hydrogeological structures which jointly with topography control transport.

REFERENCES

Alvarez, P.J. & Illman, W.A. (2005). *Bioremediation and natural attenuation: process fundamentals and mathematical models*, volume 27. John Wiley & Sons.

Benettin, P., Kirchner, J.W., Rinaldo, A. & Botter, G. (2015). Modeling chloride transport using travel time distributions at Plynlimon, Wales. *Water Resources Research*, 51(5):3259–3276.

Beven, K. (2001). Dalton Medal lecture: How far can we go in distributed hydrological modelling? *HESS*, (5):1–12.

Beven, K. (2009). Environmental Modelling: An Uncertain Future? *Routledge, London, U.K.*, p. 310 pp.

Beven, K. (1989). Changing ideas in hydrology-The case of physically-based models. *Journal of Hydrology*, 105:157 – 172. doi:http://dx.doi.org/10.1016/0022-1694(89)90101-7.

Bosson, E., Sassner, M., Sabel, U. & Gustafsson, L.G. (2010). Modelling of present and future hydrology and solute transport at Forsmark. SR-Site Biosphere. Technical report, Swedish Nuclear Fuel and Waste Management Co., Stockholm (Sweden).

Botter, G., Bertuzzo, E. & Rinaldo, A. (2011). Catchment residence and travel time distributions: The master equation. *Geophysical Research Letters*, 38(11).

Butts, M. & Graham, D. (2005). Evolution of an integrated surface water-groundwater hydrological modelling system.

Butts, M.B., Payne, J.T., Kristensen, M. & Madsen, H. (2004). An evaluation of the impact of model structure on hydrological modelling uncertainty for streamflow simulation. *Journal of Hydrology*, 298:242 – 266. doi:http://dx.doi.org/10.1016/j.jhydrol.2004.03.042. The Distributed Model Intercomparison Project (DMIP).

Cardenas, M.B. (2007). Potential contribution of topography-driven regional groundwater flow to fractal stream chemistry: Residence time distribution analysis of Tóth flow. *Geophysical Research Letters*, 34(5).

Carrera, J., Sánchez-Vila, X., Benet, I., Medina, A., Galarza, G. & Guimerà, J. (1998). On matrix diffusion: formulations, solution methods and qualitative effects. *Hydrogeology Journal*, 6(1):178–190.

Cornaton, F. (2012). Transient water age distributions in environmental flow systems: The time-marching Laplace transform solution technique. *Water Resources Research*, 48(3).

Cvetkovic, V., Cheng, H. & Wen, X.H. (1996). Analysis of nonlinear effects on tracer migration in heterogeneous aquifers using Lagrangian travel time statistics. *Water Resources Research*, 32(6):1671–1680. doi:10.1029/96WR00278.

Cvetkovic, V., Fiori, A. & Dagan, G. (2016). Tracer travel and residence time distributions in highly heterogeneous aquifers: Coupled effect of flow variability and mass transfer. *Journal of Hydrology*. doi:http://dx.doi.org/10.1016/j.jhydrol.2016.04.072.

Cvetkovic, V. (2011a). The tempered one-sided stable density: a universal model for hydrological transport? *Environmental Research Letters*, 6(3):034008.

Cvetkovic, V. (2011b). Tracer attenuation in groundwater. *Water resources research*, 47(12).

Cvetkovic, V., Carstens, C., Selroos, J.O. & Destouni, G. (2012). Water and solute transport along hydrological pathways. *Water Resources Research*, 48(6):n/a–n/a. doi:10.1029/2011WR011367. W06537.

Cvetkovic, V., Soltani, S. & Vigouroux, G. (2015). Global sensitivity analysis of groundwater transport. *Journal of Hydrology*, 531:142–148.

Darracq, A., Destouni, G., Persson, K., Prieto, C. & Jarsjö, J. (2010). Scale and model resolution effects on the distributions of advective solute travel times in catchments. *Hydrological processes*, 24(12):1697–1710.

Darracq, A., Lindgren, G. & Destouni, G. (2008). Long-term development of Phosphorus and Nitrogen loads through the subsurface and surface water systems of drainage basins. *Global Biogeochemical Cycles*, 22(3).

Darracq, A. & Destouni, G. (2007). Physical versus biogeochemical interpretations of nitrogen and phosphorus attenuation in streams and its dependence on stream characteristics. *Global Biogeochemical Cycles*, 21(3):n/a–n/a. doi:10.1029/2006GB002901. GB3003.

Destouni, G. & Graham, W. (1995). Solute transport through an integrated heterogeneous soil-groundwater system. *Water resources research*, 31(8):1935–1944.

Destouni, G., Persson, K., Prieto, C. & Jarsjö, J. (2010). General quantification of catchment-scale nutrient and pollutant transport through the subsurface to surface and coastal waters. *Environmental science & technology*, 44(6):2048–2055.

Engdahl, N.B. & Maxwell, R.M. (2014). Approximating groundwater age distributions using simple streamtube models and multiple tracers. *Advances in Water Resources*, 66:19–31.

Engdahl, N.B. & Maxwell, R.M. (2015). Quantifying changes in age distributions and the hydrologic balance of a high-mountain watershed from climate induced variations in recharge. *Journal of Hydrology*, 522:152–162.

Fiori, A., Russo, D. & Di Lazzaro, M. (2009). Stochastic analysis of transport in hillslopes: Travel time distribution and source zone dispersion. *Water Resources Research*, 45(8):n/a–n/a. doi:10.1029/2008WR007668. W08435.

Fiori, A. & Russo, D. (2008). Travel time distribution in a hillslope: Insight from numerical simulations. *Water Resources Research*, 44(12).

Ginn, T.R. (1999). On the distribution of multicomponent mixtures over generalized exposure time in subsurface flow and reactive transport: Foundations, and formulations for groundwater age, chemical heterogeneity, and biodegradation. *Water Resources Research*, 35(5):1395–1407. doi:10.1029/1999WR900013.

Goderniaux, P., Davy, P., Bresciani, E., de Dreuzy, J.R. & Le Borgne, T. (2013). Partitioning a regional groundwater flow system into shallow local and deep regional flow compartments. *Water Resources Research*, 49(4):2274–2286. doi:10.1002/wrcr.20186.

Goode, D.J. (1996). Direct Simulation of Groundwater Age. *Water Resources Research*, 32(2):289–296. doi:10.1029/95WR03401.

Gotovac, H., Cvetkovic, V. & Andricevic, R. (2009). Flow and travel time statistics in highly heterogeneous porous media. *Water Resources Research*, 45(7):n/a–n/a. doi:10.1029/2008WR007168. W07402.

Graham, D.N. & Butts, M.B. (2005). Flexible, integrated watershed modelling with MIKE SHE. *Watershed models*, 849336090:245–272.

Haggerty, R. & Gorelick, S.M. (1995). Multiple-rate mass transfer for modeling diffusion and surface reactions in media with pore-scale heterogeneity. *Water Resources Research*, 31(10):2383–2400.

Haggerty, R., McKenna, S.A. & Meigs, L.C. (2000). On the late-time behavior of tracer test breakthrough curves. *Water Resources Research*, 36(12):3467–3479. doi:10.1029/2000WR900214.

Haitjema, H. (1995). On the residence time distribution in idealized groundwatersheds. *Journal of Hydrology*, 172(1):127 – 146. doi:http://dx.doi.org/10.1016/0022-1694(95)02732-5.

Kirchner, J.W., Feng, X. & Neal, C. (2000). Fractal stream chemistry and its implications for contaminant transport in catchments. *Nature*, 403(6769):524–527.

Kirchner, J.W., Feng, X. & Neal, C. (2001). Catchment-scale advection and dispersion as a mechanism for fractal scaling in stream tracer concentrations. *Journal of hydrology*, 254(1):82–101.

Lindgren, G.A. & Destouni, G. (2004). Nitrogen loss rates in streams: Scale-dependence and upscaling methodology. *Geophysical Research Letters*, 31(13):n/a–n/a. doi:10.1029/2004GL019996. L13501.

Lindgren, G.A., Destouni, G. & Miller, A.V. (2004). Solute transport through the integrated groundwater-stream system of a catchment. *Water Resources Research*, 40(3):n/a–n/a. doi:10.1029/2003WR002765. W03511.

Loague, K. & VanderKwaak, J.E. (2004). Physics-based hydrologic response simulation: platinum bridge, 1958 Edsel, or useful tool. *Hydrological Processes*, 18(15):2949–2956. doi:10.1002/hyp.5737.

Małoszewski, P., Rauert, W., Stichler, W. & Herrmann, A. (1983). Application of flow models in an alpine catchment area using tritium and deuterium data. *Journal of Hydrology*, 66(1):319–330.

Małoszewski, P. & Zuber, A. (1982). Determining the turnover time of groundwater systems with the aid of environmental tracers: 1. Models and their applicability. *Journal of hydrology*, 57(3-4):207–231.

Maloszewski, P. & Zuber, A. (1996). Lumped parameter models for the interpretation of environmental tracer data. Technical report.

McDonnell, J.J., McGuire, K., Aggarwal, P., Beven, K.J., Biondi, D., Destouni, G., Dunn, S., James, A., Kirchner, J., Kraft, P., Lyon, S., Maloszewski, P., Newman, B., Pfister, L., Rinaldo, A., Rodhe, A., Sayama, T., Seibert, J., Solomon, K., Soulsby, C., Stewart, M., Tetzlaff, D., Tobin, C., Troch, P., Weiler, M., Western, A., Wörman, A. & Wrede, S. (2010). How old is streamwater? Open questions in catchment transit time conceptualization, modelling and analysis. *Hydrological Processes*, 24(12):1745–1754. doi:10.1002/hyp.7796.

McGuire, K.J. & McDonnell, J.J. (2006). A review and evaluation of catchment transit time modeling. *Journal of Hydrology*, 330:543 – 563. doi:http://dx.doi.org/10.1016/j.jhydrol.2006.04.020.

McGuire, K., McDonnell, J.J., Weiler, M., Kendall, C., McGlynn, B., Welker, J. & Seibert, J. (2005). The role of topography on catchment-scale water residence time. *Water Resources Research*, 41(5).

Meinardi, C., Beusen, A., Bollen, M., Klepper, O. & Willems, W. (1995). Vulnerability to diffuse pollution and average nitrate contamination of European soils and groundwater. *Water Science and Technology*, 31(8):159–165.

Montgomery, D.R. & Foufoula-Georgiou, E. (1993). Channel network source representation using digital elevation models. *Water Resources Research*, 29(12):3925–3934.

Nielsen, P.H., Bjerg, P.L., Nielsen, P., Smith, P. & Christensen, T.H. (1995). In situ and laboratory determined first-order degradation rate constants of specific organic compounds in an aerobic aquifer. *Environmental science & technology*, 30(1):31–37.

Niemi, A.J. (1977). Residence time distributions of variable flow processes. *The International Journal of Applied Radiation and Isotopes*, **28**(10):855 – 860. doi:http://dx.doi.org/10.1016/0020-708X(77)90026-6.

Noolandi, J. (1977). Multiple-trapping model of anomalous transit-time dispersion in a- S e. *Physical Review B*, **16**(10):4466.

Refsgaard, J.C., van der Sluijs, J.P., Brown, J. & van der Keur, P. (2006). A framework for dealing with uncertainty due to model structure error. *Advances in Water Resources*, **29**(11):1586 – 1597. doi:http://dx.doi.org/10.1016/j.advwatres.2005.11.013.

Rinaldo, A., Beven, K.J., Bertuzzo, E., Nicotina, L., Davies, J., Fiori, A., Russo, D. & Botter, G. (2011). Catchment travel time distributions and water flow in soils. *Water resources research*, **47**(7).

Rodhe, A., Nyberg, L. & Bishop, K. (1996). Transit Times for Water in a Small Till Catchment from a Step Shift in the Oxygen 18 Content of the Water Input. *Water Resources Research*, **32**(12):3497–3511. doi:10.1029/95WR01806.

Tetzlaff, D., Seibert, J., McGuire, K., Laudon, H., Burns, D., Dunn, S. & Soulsby, C. (2009). How does landscape structure influence catchment transit time across different geomorphic provinces? *Hydrological Processes*, **23**(6):945–953.

Toth, J. (1963). A theoretical analysis of groundwater flow in small drainage basins. *Journal of geophysical research*, **68**(16):4795–4812.

Troldborg, L., Jensen, K.H., Engesgaard, P., Refsgaard, J.C. & Hinsby, K. (2008). Using Environmental Tracers in Modeling Flow in a Complex Shallow Aquifer System. *Journal of Hydrologic Engineering*, **13**(11):1037–1048. doi:10.1061/(ASCE)1084-0699(2008)13:11(1037).

Varni, M. & Carrera, J. (1998). Simulation of groundwater age distributions. *Water Resources Research*, **34**(12):3271–3281.

Weissmann, G.S., Zhang, Y., LaBolle, E.M. & Fogg, G.E. (2002). Dispersion of groundwater age in an alluvial aquifer system. *Water Resources Research*, **38**(10).

Woolfenden, L.R. & Ginn, T.R. (2009). Modeled ground water age distributions. *Groundwater*, **47**(4):547–557.

Wörman, A., Packman, A.I., Marklund, L., Harvey, J.W. & Stone, S.H. (2006). Exact three-dimensional spectral solution to surface-groundwater interactions with arbitrary surface topography. *Geophysical research letters*, **33**(7).

Xu, C.y. (2003). Testing the transferability of regression equations derived from small sub-catchments to a large area in central Sweden. *Hydrology and Earth System Sciences Discussions*, **7**(3):317–324.

OTHER REFERENCES

©DHI-WASY GmbH (2012), *FEFLOW 6.2*, `https://www.mikepoweredbydhi.com/products/feflow`.

Lantmäteriet (2012). Höjddata grid 50+ nh, raster ©Lantmäteriet. Data retrieved from SLU (Swedish University of Agricultural Sciences) database, `https://zeus.slu.se/get/?drop=`.

SGU (2016). Swedish Geological Survey, Jorddjupdata, raster ©SGU. Data retrieved from SLU (Swedish University of Agricultural Sciences) database, `https://zeus.slu.se/get/?drop=`.

SLU (2012). Miljödata, ©MVM. Data retrieved from SLU (Swedish University of Agricultural Sciences) database, http://miljodata.slu.se/mvm.

SMHI (2012). Swedish Meteorological Hydrology Institute, Precipitation data, ©SMHI. Data retrieved from SMHI (Swedish Meteorological Hydrology Institute) database, https://www.smhi.se/klimatdata/meteorologi/nederbord.

SMHI (2012). Swedish Meteorological Hydrology Institute, Lakes and rivers data, ©SMHI. Data retrieved from SMHI (Swedish Meteorological Hydrology Institute) database, https://www.smhi.se/klimatdata/hydrologi/svenskt-vattenarkiv.

SMHI (2012). Swedish Meteorological Hydrology Institute, River discharge data, ©SMHI. Data retrieved from SMHI (Swedish Meteorological Hydrology Institute) database, https://www.smhi.se/klimatdata/hydrologi/vattenforing.